



Thermal Dislocation and Physical Changes During Preparation of Active Silicate of Group 2 Periods 3, 4 and 5 Elements from Spent Fines of Finishing Crystal Glass

Mahmoud Abdelhamed Rabah*

Chemical and electrochemical treatment, Mineral Processing Dept. Central Metallurgical Research and Development Institute, CMRDI P.O.Box 87 Helwan 11421 Cairo, Egypt

ARTICLE INFO

Received: 19 March 2019
Revised: 10 April 2019
Accepted: 20 April 2019
Available online: 22 April 2019

DOI: 10.33945/SAMI/AJCA.2019.4.3

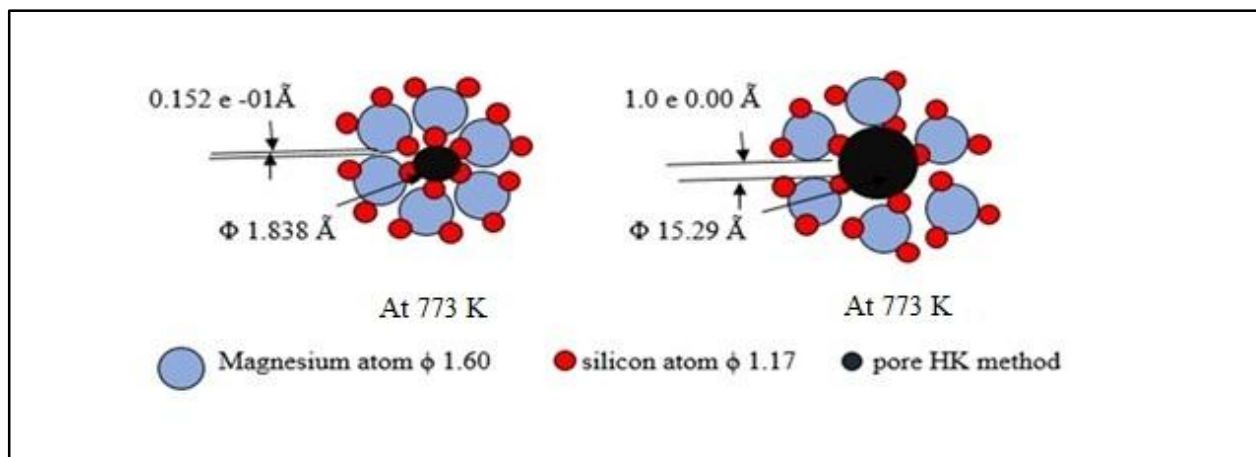
KEYWORDS

Lead oxide(s)
Hydrometallurgy
Magnesium metasilicate
Surface adsorption

ABSTRACT

This study reports on the thermal dislocation and crystal growth changes during preparation of active metasilicate of group 2 periods 3, 4 and 5 elements from waste fines of finishing process of crystal glass (CG) industry. Sodium carbonate fused the fines at ≈ 1273 K for 120-180 minutes followed by water leaching. Alkali silicate goes into solution. Primary chloride and sulphate salts of elements of group 2 periods 2, 4 and 5 added to the alkali silicate solution at temperatures 300 K to 353 K for 60 minutes to give metasilicate as a white precipitate followed by heating at 473 K to 1073 K for 30 minutes. The study discussed the physical changes taking place after heating. Results revealed that surface area and adsorption capacity of Mn ions from underground water increased with the surface area of the silicate associating the decrease in atomic radius of the element. The effect of pH, concentration of the reactants and temperature on the synthesis and physical changes of the silicate salts has been investigated. Formation of the silicate salt proceeded in a reaction sequence involving atom rearrangement to form a honeycomb structure with very narrow pore diameter amounting to 1.538 Å. Heating silicate at 773 K dislocate the oxygen atoms around metal atoms to form unit crystals with mild pore diameter of 15.29 Å. With further increase in temperature, narrow pore system collapses to form sponge structure with wider pore diameter and lower surface area. The manuscript tabulated the physical changes in digital presentation derived mathematically.

GRAPHICAL ABSTRACT



* Corresponding author's E-mail address:

mrabah010@gmail.com, mahmoudrabah2@hotmail.com

Introduction

Sodium carbonate powder is a fusing agent; sodium sulfide is a catalytic agent while carbon powder acts as a reducing material. Practical experience showed that lead recovery increased with the increase in the weight ratio of the added sodium carbonate and sodium sulfide, temperature and holding time. The maximum extent of lead recovery amounts to nearly 94% by using the optimum amount of sodium carbonate together with sodium sulfide at temperature 1200 °C for 120 min. In the melting process exercised at high temperature, lead silicate in funnel glass firstly reduced, and then removed. The glass slag can be processed to give sodium and potassium silicate by chemical process. That study proposed a practical and economical process for recovery of lead and utilization of waste glass slag [1]. The difficulty of treating waste CRT funnel glass is the complexity of structure of CRT glass. The lattice of the glass network of crystal glass captured lead atoms and partly formed other structure component of the glass network such as SiO_2PbO [2]. Lead oxide is tightly captured in silica tetrahedron hindering the leaching efficiency of lead [3]. However, several approaches had been investigated for lead recovery from Spent crystal glass. These methods were processes of pretreatment, chemical leaching and thermal reduction [5] at high temperatures. Pretreatment included mechanical activation method [6,7], subcritical water [8] and chemical leaching [9] enhanced by ultrasonic waves. However, such process gave low recovery extent and required long time, high-energy consumption and additional thermal agents. The leaching solution contained water, acid [10,11] and alkalis [12]. Some thermal process included reduction under vacuum, chloride volatilization [13-15] and hydrothermal sulphidization [16]. Nevertheless, these technologies still have some disadvantages, such as harsh reaction

condition, the other components in the glass are not effectively utilized, lack of economic feasibility, and too complicated for industrial production

In a previous study [17], the efficiency of lead extraction from spent leaded glass in strongly alkaline solution was evaluated after mechanical activation in a planetary ball mill as a chemical breakage of defects formed in the inner structure. The authors reported that would contribute to the easy dissolution of the activated leaded glass. Studies reported the influence of rotation speed, time of mechanical activation, sodium hydroxide concentration, leaching temperature and phase ratios (v/w). Mechanical activation gave more than 78% of lead extraction compared to 3.5% lead extraction extent for chemical leaching of non-activated samples. Electro winning of lead from the leaching solution gave high purity lead powder. According to a US Patent [18], lead-depleted solution could be recycled into the leaching step. A hydrometallurgical process for has reported recovering lead from spent leaded glass in alkaline solution. There had described a process completely performed in aqueous phase, provided a heat etching of lead glass with aqueous solutions of strong alkali followed by electrolysis of the suspension so formed. This was to recover metallic lead and obtain soluble silicates.

Aris Erzat and Fu-Shen Zhang reported a technological method [19] in which the glass powder was first compressed into cylindrical pellet homogeneously mixed with a chlorinating agents. Solid-phase reactions took place by heating the pellets. In that case, the silicon oxide network of the glass gave lead metal. Lead chloride was the product. Studies found that lead chloride was the most effective chlorinating agent, and the optimum operation temperature, holding time and system pressure were 1000 °C, 2 h, 600 ± 50 Pa, respectively. PbCl_2 produced from the system easily recovered by cooling. The

extent of lead recovery from waste CRT amounted to 99.1% with a purity extent of the recovered PbCl_2 of 97.0%. The process identified the reaction mechanism. Huang *et al.* (2018) reported the use of Mg silicate as an effective adsorbent material for removal of Zn and Cu from wastewater [20]. Stephen Mg Silicate has adsorption capacity of 198 mg Zn /g silicate and 113.5 mg Cu. In 2017, Huang *et al.* showed that porous Mg silicate has an adsorption capacity of 78-86 mg Zn and 52-30 mg Cu/g Mg silicate [21]. Stephen Earle [22] reported the ionic radii of some elements usually found in silicate compounds. The ionic radius of oxygen, calcium, magnesium and strontium are 1.4, 1.00, 0.97 and 0.74 Å. In addition, it was found [22] that the effect of ionic radius on hardness is opposite for alkali and alkaline earth ions. The effect of composition on the hardness of structured network occurring at the atomic scale is considered. Heating improved the structural density of glasses and increase hardness. For silicate of alkali ions, structural density increases with increasing ionic radius, whereas for alkaline earth ions the opposite effect took place [22].

The aim of this study postulates the effect of heat treatment on the structure, crystal growth and physical changes of active silicate of group 2 periods 3, 4 and 5 elements

synthesized from waste fines purged from finishing process of crystal glass. The applied process of synthesis discussed some physical parameters that have influence to elucidate these changes.

Experimental

Materials and Methods

The fines of crystal glass

About 2 kg of the fines generating from the polishing process of crystal glass manufacturing in industrial plant in Cairo was obtained from the waste yard, about 200 m apart from the plant location at Shoubra El Khema, Cairo Egypt. Size classification of the sample by sieving gave four cuts having the sizes as shown in Table 1.

The underground water

Table 2 shows the specifications of a sample of underground water taken shallow depth ($\approx 9\text{m}$) from Nazlet El Samman region, Al Ahram, Giza.

The Chemicals

Table 3 shows the properties of the chemicals used in this work.

Table 1. Particle size distribution of the crystal glass fines

Size, μm As received	Symbol As received	weight	
		g	%
total		2100	100
>60<100	FF	250	11.95
>100<150	F	450	21.45
>150<200	FC	600	28.5
>200	C	800	38.1

Table 2. Specifications of underground water

Property	Physical	Metal content
Color	Clear	Fe, 0.6 mg /l
Taste	Undesirable	Mn 0.9 .g/ l
Odor	Odorless	Ca 2.5 mg /l

Table 3. The properties of chemicals used

Product	Property	Purpose	Origin
CH ₃ COOH	90 %		Riedel- de Hein
	SP. Gr. 1.044 – 1.049		
Nitric acid	SP.GR.1.18 (AR)	Leaching	ADWIC
	Min. assay 36 %		
H ₂ SO ₄	Fuming 69 %	Process	Riedel- de Hein
	95-97% Extra pure		
HCl	SP.GR.1.18 (AR)		ADWIC
Na ₂ CO ₃ , EJSF2	99.3, 1.6 um		Sigma Aldrich
NaOH	Pure reagent		United Co.
NH ₄ OH	25 % Pure reagent		
AgNO ₃	Pure reagent	Chloride ion determination	
Mono-distilled water		Chemical reactions	
Tap water		Other purposes	

Adsorption Experiments

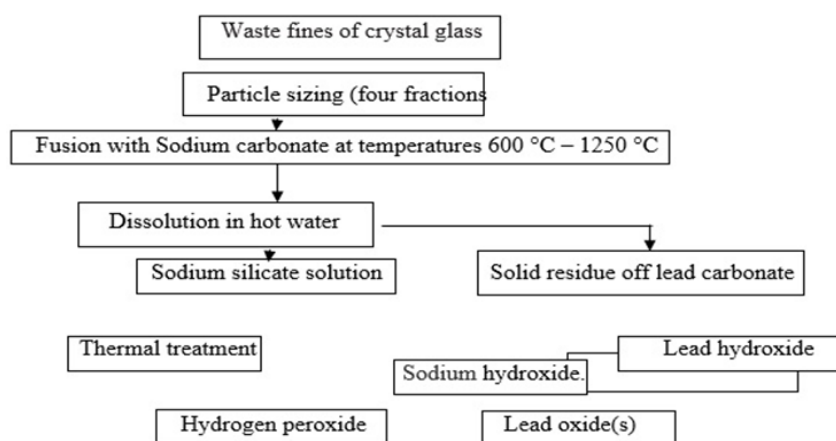
The adsorption experiments for the determination of adsorption capacity of active silicate were using vertical column, 2 cm in diameter and 10 cm long, with inlet and outlet opening and fitted with discharge valve to control the flow rate of water. An atomic spectrophotometer type Raman-HR, 200-2750cm⁻¹ USA determined iron and Mn

content in the exit water. The column was loaded with the silicate powder and water was running at the required flow rate.

Description of the Process Flow Sheet

Figure 1 shows the sequential process flow sheet of the process applied to carry out the experiments of this study.

Figure 1. Sequential process flow sheet of the experiments



Methods of determination of physicochemical properties

Lead was determined as lead chromate.

Determination of silicate density, pore volume. Pore radius, adsorption volume and surface area were measured using Quanta chrome instrument version 11.04.

Measurement of Brownian motion and relation this to the size of the particles by using a correlation function and the Stokes-Einstein equation Non-spherical particles that were measured as equivalent spheres.

Result and Discussion

Figure 2 shows a photograph of the waste material. Table 4 shows the element content of the waste fines resulted from finishing process of the crystal glass. The major

portions are lead and silicon metals. Other earth metals are present in small weight percentage.

Figure 3 shows the effect of heating temperature for different times on the extent of recovery of alkali silicate from the waste fines of crystal glass. It can be seen that the extent of recovery increases with the corresponding increase in temperature up to 1373 K, Also, the extent of recovery increases with the increase in time of heating up to 180 minutes.

Figure 2. A photograph of waste fines of the crystal glass



Table 4. The element content of the waste fines

Element	Weight %
Pb	51.2
Si	32.47
Ca	2.24
Na	1.63
K	1.54
Al	1.35
Mg	0.37

Figure 3. Effect of heating temperature on the extent of alkali silicate recovery after fluxing with sodium carbonate

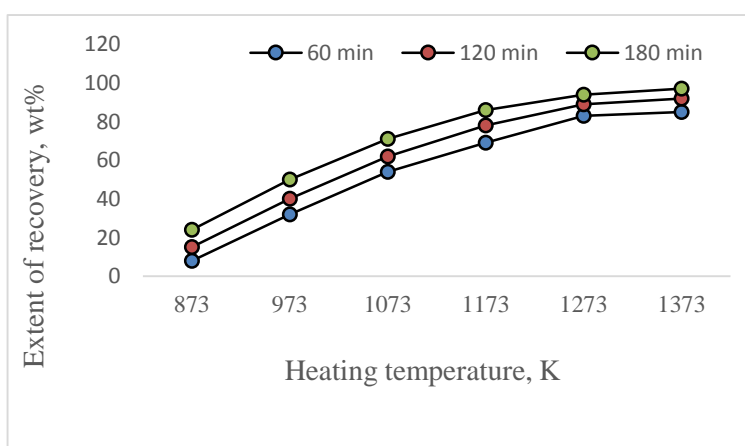


Figure 4 shows the XRD pattern of the recovered lead from the spent fines of crystal

glass it can be seen that the obtained lead oxide is almost pure.

Figure 5 shows the effect of pH value on the extent of synthesis of metasilicate salt. It is seen that the extent of synthesizing the silicate salt increases with the increase of pH value, nearly complete extent of silicate synthesis takes place at ≥ 4 . More alkalinity of the synthesis medium is in favour of synthesis

Figure 4. The XRD pattern of the recovered lead from the spent fines of crystal glass

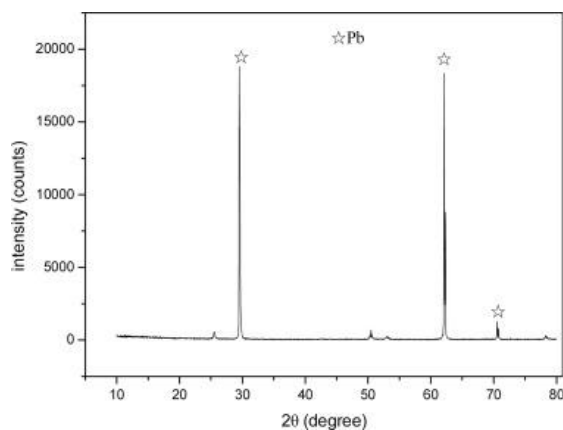


Figure 5. Effect of pH value on the extent of synthesis of metasilicate salt

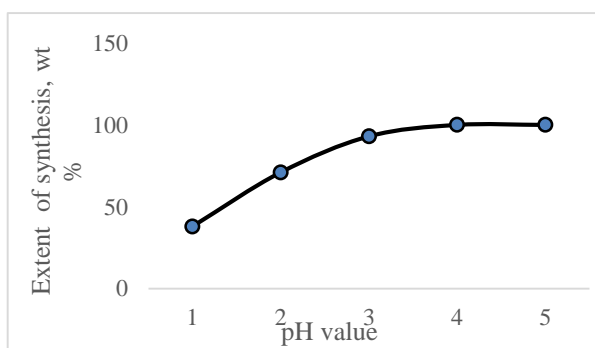


Figure 6. Effect of heating temperature on the extent of recovery of sodium silicate from the spent fines of crystal glass

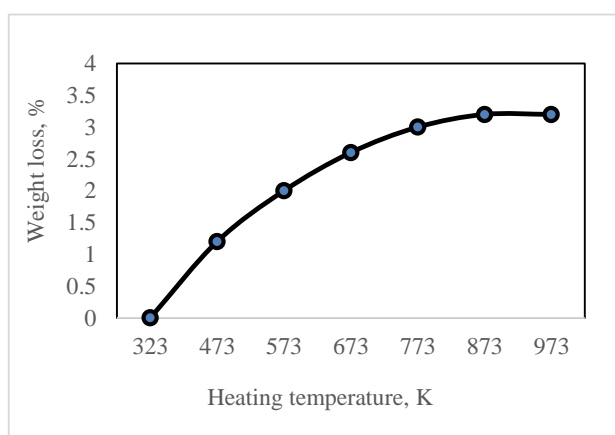


Figure 7 shows the atomic radii of magnesium, calcium and strontium metals. The mean pore diameter of the silicate compounds increases in the order Mg silicate,

the silicate, Figure 6 illustrates the effect of heating temperature on the weight loss upon heating the so formed silicate, It is seen that the extent of weight loss of the silicate slightly increases with increase in heating temperature up to its maximum at 973 K amounting to 3.2 %.

Ca silicate and Sr Silicate. Figure 8 shows the apparent density value of the prepared silicate of Mg, Ca and Sr at room temperature. The apparent density of magnesium, calcium

and strontium silicate salts in g/ml decrease in the order Mg (0.54), Ca (0.825) and Sr (0.652).

Figure 9 shows the change in apparent density value of Mg silicate, Ca silicate and Sr silicate as a function of heating temperature

Figure 7. The atomic radii of Mg, Ca and Sr elements

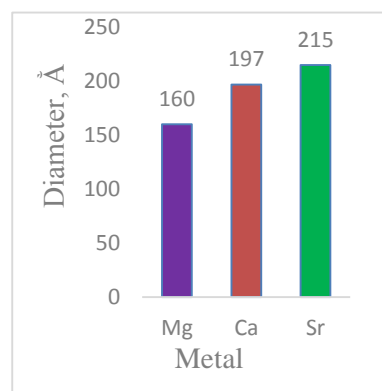


Figure 8. The density of silicate salt of Mg, Ca and Sr prepared at room temperature

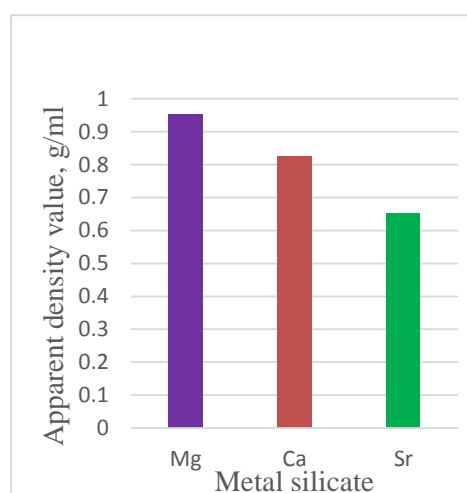


Figure 9. The apparent density of Mg, Ca and Sr silicate as a function of temperature up to 1273 K

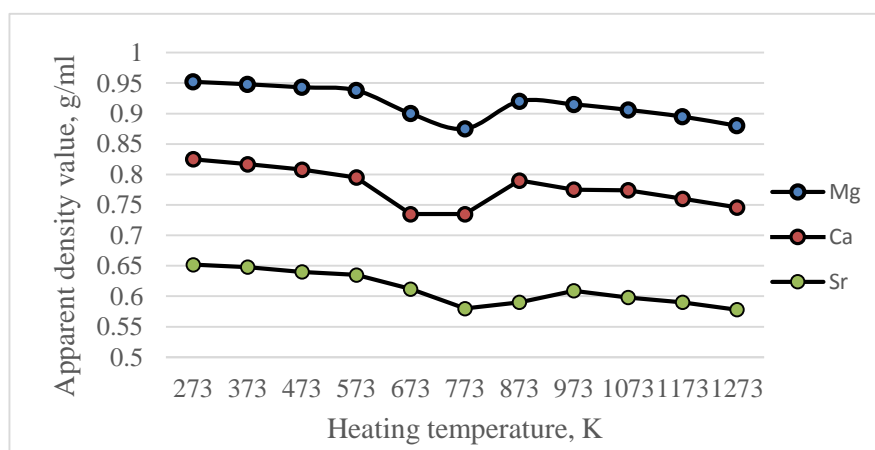


Figure 10 shows the mean pore diameter of Mg silicate as a function of heating

temperature. The pore diameter displays a parabolic shape curve. It decreases upon

heating the silicate material at 773 K attaining the minimum value. With further increase in temperature, pore diameter increases.

Figure 11 shows the mean pore diameter of M, Ca and Sr silicate as a function of heating temperature.

The pore diameter displays the same

parabolic shape curve as given in Figure 9. Pore diameter decreases upon heating the silicate material at 773 K attaining the minimum value. The pore diameter increases again with further increase in temperature up to 1073 K. It is worthy to note that pore diameter increases in the order Sr silicate, Ca silicate and Mg silicate.

Figure 10. The mean pore diameter of Mg silicate as a function of heating temperature

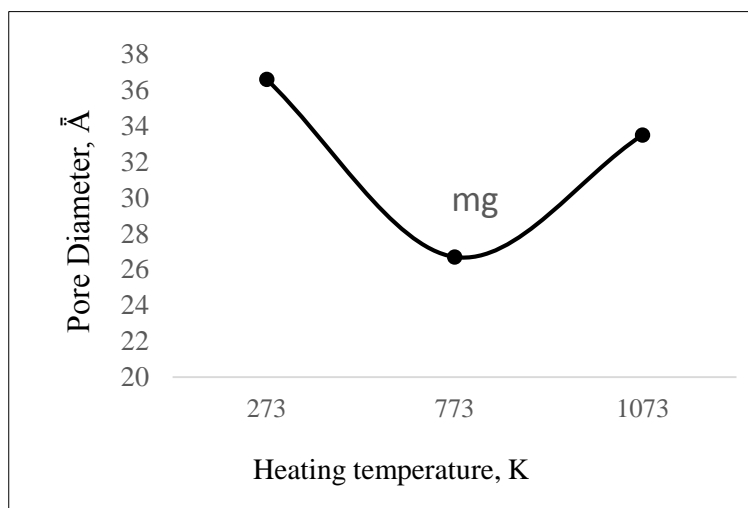


Figure 11. The mean pore diameter of Mg silicate, Ca silicate and Sr silicate as a function of heating temperature up to 1073 K

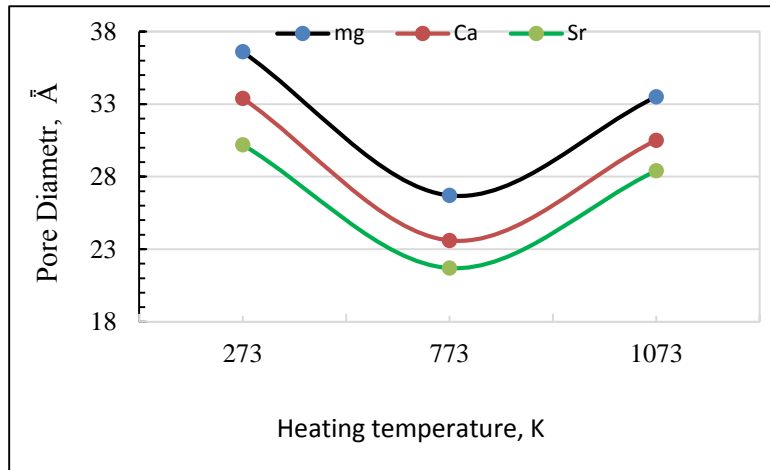


Figure 12 shows the cumulative pore-surface area of the silicate samples heated at temperatures up to 1073 K. The cumulative pore surface area of the samples after preparation and not thermally heated are of small magnitude. Surface area increases with heating passing through a maximum at 773 K and decreases with further increasing the heating temperature up to 1073 K. It is worth

noting that the surface area decreases in the order Mg, Ca and Sr silicate.

Figure 13 shows the cumulative pore volume Mg silicate as a function of heating temperature up to 1073 K. It can be seen that the cumulative pore volume has its highest volume at 773 K and displays lower volume at less or high temperatures.

Figure 12. The cumulative surface area of the silicate samples as a function of the heating temperature up to 1073 K

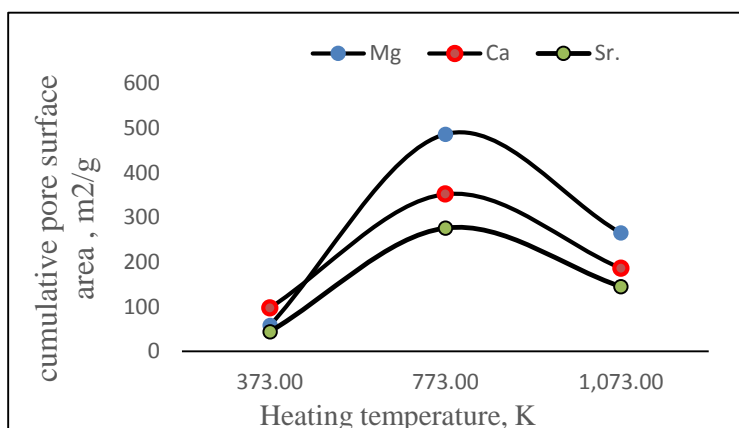


Figure 13. The cumulative pore volume of Mg silicate as a function of heating temperature

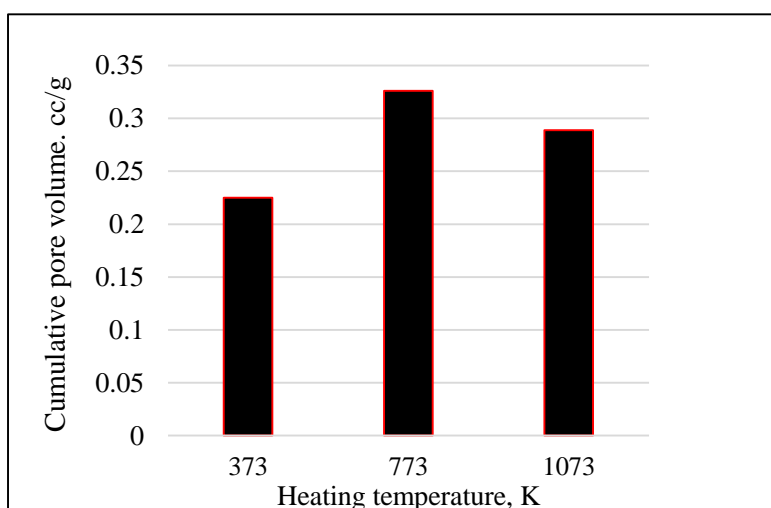


Figure 14. Adsorption extent of manganese ions from under-ground water at ambient conditions

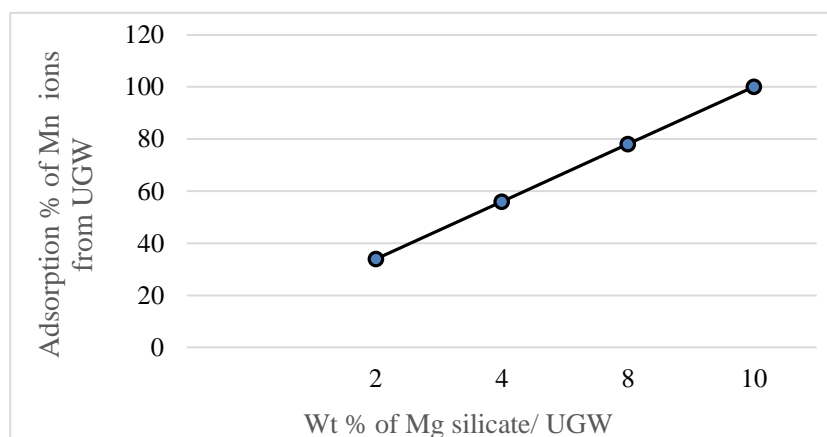


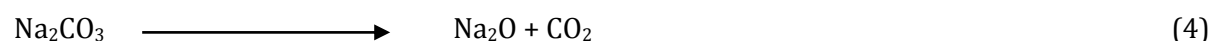
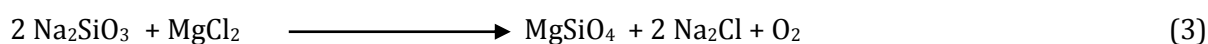
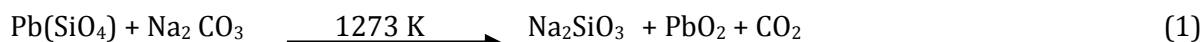
Figure 14 shows the adsorption extent of manganese ions from under-ground water (UGW) by magnesium silicate at ambient conditions. The extent of adsorption linearly related to the weight of used Mg silicate whereby complete removal of the manganese ions takes place with 10 % of the silicate used.

Discussion

The aim of this work is to prepare active silicate of Mg, Ca and Sr from waste fines of polishing process in the manufacture of crystal glass industry. Heating the waste fines with sodium carbonate at high temperature

1273 K recovered the water-soluble sodium silicate and insoluble lead oxides. Sodium silicate so obtained were reacted with aqueous solution of primary chloride or sulphate salts of Mg, Sr and calcium to give the respective silicate of these metals.

Sodium silicate so obtained reacted with primary metal chloride or sulphate to form



In addition, reaction (3) is the overall reaction of equations 4 and 5.

In this context, the effect of pH justifies that water-soluble lead compounds predominates at higher pH values are water insoluble in low pH values (6-11). Changes in Physical structure easily takes place with soluble lead ions and became hard to display the same effect with insoluble lead compounds.

Silicate molecule is structured from a silicon atom bonded with three (ortho silicate) or four oxygen atoms (tetrahedron metasilicate). The distance between silicon and oxygen amounts to 0.163 nm and between two adjacent oxygen atoms 0.264 nm. Oxygen atoms structured with an angle amounting to 109.28°. Measurements of molecular size of magnesium, calcium and strontium silicate showed that it is 1.64 nm, 1.86 and 2.05 nm respectively.

The separating force (F) follows the law for Coulomb force between negatively q_1 and positively charged q_2 ions (oxygen and silicon) as calculated from the relation force changes as a function of the square of the distance separation between charges.

metal silicate and sodium chloride or sulphate.

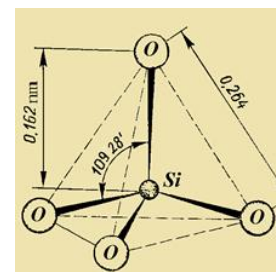
Reaction (3) is the overall reaction of sequence taking place as follows:

NaCO_3 decomposes upon heating at $\geq 1073\text{ K}$ to sodium oxide and CO_2 .

Lead sulfate (PbSiO_4) reacts with sodium oxide to give sodium silicate and lead oxide.

$$F = k \frac{q_1 q_2}{r^2} \quad (6)$$

Figure 15. The structure of silicate molecule



Silicate molecule structured from six silicate units with a pore at the core. Mathematical computation of the size of one silicate molecule was derived as follows. The diameter of metal atom + radius of oxygen atom, + the distance between oxygen and metal atom = $0.168 + 0.66 + 1.60$ (with Mg atom) = 2.428 \AA . It follows that the size of silicate molecule amounts to $6 * 2.428 + 6 * 0.0152 + \text{pore diameter } (1.838) = 15.417.2\text{ \AA} = 0.015417\text{ nm}$ (Figure 16).

The effect of heating has physical changes on the silicate structure involving atom dislocation of the oxygen atoms around the silicon atom. This effect was confirmed from the density value that do not change by

heating up to 1273 K in contrary to the explanation reported by Smedskjaer [22].

Our measurements showed that the pore radii of Mg silicate increases with increase in heating temperature and the interatomic

distance also increases from 0.0152 Å to 1.000 Å and the pore diameter increases from 1.838 Å to 15.32 Å to form the following structure(Figure 17).

Figure 16. The structure of silicate molecule

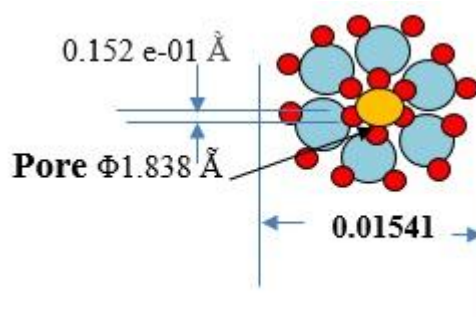
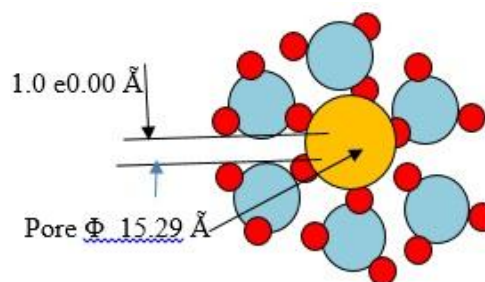


Figure 17. The effect of heating on the silicate structure



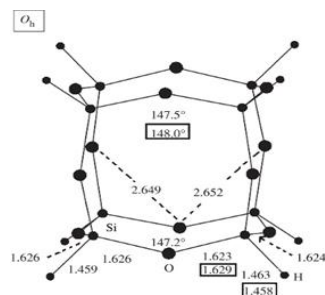
This postulation finds support from the following experimentally found results. The density did not change upon heating from 573 up to 1073 K (Figure 9). However, The decrease-taking place with density value at 773 K resulted from the corresponding increase in pore volume (Figure 13). The development that takes place with density (Figure 9), the pore radii (Figure 10) and adsorption surface area that increase with increase in temperature can be explained to the physical thermal expansion of the unit cells of silicate and not to the weight loss of material. However, the loss in weight seen by heating the silicate samples up to 573 K was due to the thermal vaporization of residual moisture content in the silicate crystals. Heating at higher temperatures do not display any loss in weight (Figure 6). A sample of heated Mg silicate has proven successful to remove polluting Mn ions from underground

water. Results revealed that the silicate sample was suitable to adsorb Mn ions and complete removal of these ions takes place with about 10 % by weight silicate in underground water. The adsorption capacity of Mg silicate to adsorb Mn ions from underground water amounts to 98 mg Mn/g silicate. Crystallographic faces studies of the silicate molecule as given by Schutte and Pretorius [23]. The name referring to its almost spherical O_h shape is one of the most interesting silicates that has Si-H bonds. The molecule can be considered a three-dimensional octahedral polymer; its experimentally determined molecular structure is diagrammatic (Figure 18).

The main reason for the small elongation of the linear dimensions of the unit cell is found in the opening up of the Si-O-Si-angle from approximately 147° by about $5-10^\circ$, respectively, together with the lengthening of

Figure18.

Crystallographic
face of silicate
molecule(O_h)



The non-bonded $O \cdots O$ distances by about 0.3 \AA . The reason for this might be that the computed calculation using IBM computer Mede A- fitted with special reference program (v. 4.6.36) VASP with the generalized gradient approximation (GGA). Functional under-emphasizes the extent of the charge transfer taking place between Si and O when they form a specific Si–O bond in a molecule. Hence. Causes a slightly more open Si–O–Si bond with slightly longer Si–O distance. This discrepancy almost disappears when the Pseudo-functional used in the crystal structure optimization by VASP v. 5.2, where the Si–O distances become 1.6285 and 1.6314 \AA , respectively. The Si–O–Si inter-bond angle is reduced to 146.7° , which is very much nearer to the experimental angle.

Conclusion

Waste fines of crystal glass contains recoverably sodium silicate. From this silicate solution, magnesium, calcium and strontium silicate were successfully prepared. Preparation of the synthesized silicate salts involved washing, drying and heating at temperatures up to 1273 K . The effect of thermal treatment on the physical structure of these silicate compounds proved that heating did not impart loss in material but caused changes in atomic reforming. The inter-atomic spacing between silicate units increased from 0.0152 \AA to 1.00 \AA . The pore diameter of the silicate molecule increased from 1.676 \AA to 15.9 \AA . Structural changes increased with the increase in atomic radii of the element. The

heated silicate of magnesium was suitable to remove Mn ions from underground water with a capacity of 98 mg Mn/g silicate.

Acknowledgment

The author acknowledge the unfailing help of Eng. Omar Helmy for carrying out part of the experimental study and the staff members of the Technical service Dept. Mrs Hoda Taha and her coworkers at CMRDI for providing the physical analysis.

References

- [1]. D. Hu, W. Hui, *J. Hazard. Mater.*, **2018**, 343, 220-226.
- [2]. F.O. Méar, P.G. Yot, A.V. Kolobov, M. Ribes, M.F. Guimon, D. Gonbeau, *J. Non Cryst. Sol.*, **2007**, 353, 4640-4646.
- [3]. P.G. Yot, F.O. Marled, *J. Hazard. Mater.*, **2009**, 172, 117-123.
- [4]. X. Lu, K. Shih, C. Liu, F. Wang, *Environ. Sci. Technol.*, **2013**, 47, 9972-9978.
- [5]. Q. Tan, J. Li, *Environ. Sci. Technol.*, **2015**, 49, 5849-5861.
- [6]. N. Singh, J. Li, *J. Clean. Prod.*, **2017**, 148, 103-110.
- [7]. H. Miyoshi, D.P. Chen, T. Akai, *Chem. Lett.*, **2004**, 33, 956-957.
- [8]. A.J. Saterlay, S.J. Wilkins, R.G. Compton, *Green Chem.*, **2001**, 3, 149-155.
- [9]. X. Mingfei, W. Yaping, L. Jun, X. Hua, *J. Hazard. Mater.*, **2016**, 305, 51-58.
- [10]. M. Xing, F.S. J. *Hazard. Mater.*, **2011**, 194, 407-413.
- [11]. C. Zhang, J. Wang, J. Bai, J. Guan, W. Wu, C. Guo, *Waste Manag. Res.*, **2013**, 31, 759-763.
- [12]. G. Grause, K. Takahashi, T. Kameda, T. Yoshioka, *Thermochim. Acta*, **2014**, 596, 49-55.
- [13]. G. Grause, N. Yamamoto, T. Kameda, T. Yoshioka, *Int. J. Environ. Sci. Technol.*, **2013**, 11, 959-966.
- [14]. A. Erzat, F.S. Zhang, *Environ. Technol.*, **2014**, 35, 2774-2780.
- [15]. W. Yuan, W. Meng, J. Li, C. Zhang, Q.

Song, J. Bai, J. Wang, Y. Li, *Waste Manag. Res.*, **2015**, 33, 930-936.

[16]. W. Yuan, J. Li, Q. Zhang, F. Saito, B. Yang, *J. Air Waste Manag. Assoc.*, **2013**, 63, 418-423.

[17]. J. Li, H. Hu, *Appl. Mechan. Mater.*, **2015**, 768, 441-446.

[18]. G. Modica, "Hydrothermal process for the treatment of lead glass with recovery of lead metal, soluble and insoluble silicates and silica" U.S. Patent Application 15/079,497, filed September 28, **2017**.

[19]. A. Erzat, F.S. Zhang, *J. Environ. Technol.*, **2014**, 35, 2774-2780.

[20]. R. Huang, L. He, T. Zhang, D. Li, P. Tang, Y. Feng, *ACS Appl. Mater. Interfaces*, **2018**, 10, 22776-22785.

[21]. R. Huang, M. Wu, T. Zhang, D. Li, P. Tang, Y. Feng, *ACS sustainable chem. Eng.*, **2017**, 5, 2774-2780.

[22]. M.M. Smedskjaer, M. Jensen, Y. Yue, *J. Non-Cryst. Sol.*, **2010**, 356, 893-897.

[23]. C.J.H. Schutte, J.A. Pretorius, *Proc. Royal Soc. A*, **2010**, 467, 928-953.

How to cite this manuscript: Mahmoud A. Rabah. Thermal Dislocation and Physical Changes During Preparation of Active Silicate of Group 2 Periods 3, 4 and 5 Elements from Spent Fines of Finishing Crystal Glass. *Adv. J. Chem. A*, **2019**, 2(4), 283-295.